J Appl Electrochem (2010) 40:277–284
DOI 10.1007/s10800-009-9971-6

ORIGINAL PAPER

Effects of cathode impedance on the performances of power-oriented lithium ion batteries

Yi-Shiun Chen · Chi-Chang Hu · Yuan-Yao Li

Received: 22 September 2008 / Accepted: 17 August 2009 / Published online: 30 August 2009

Abstract Since power batteries have different requirements than traditional energy-oriented lithium ion batteries (LIBs) and their design concept is also different than energy-type cells, some new problems not encountered in energy-oriented LIBs must be carefully considered. This study illustrates that cathode impedance, a contributor to total cell impedance which can be ignored in the traditional energy-type LIBs, plays a very important role in power cells. This study uses 18650 cylindrical power cells consisting of a $LiMn_2O_4$ cathode and graphite anode with a basic electrolyte of PC/EC/DMC = 1/3/6 by weight containing 1.2 M $LiPF_6$ as model power LIBs. This study also investigates the charge–discharge performance of these model batteries made from cathodes with the same recipe but dried at different oven temperatures. The high impedance cathode produced under a high drying temperature causes the cell to fail during high-power applications. Cell heating during extreme high rate discharging periods not only causes pore closure in the porous separator, but also cathode peeling from the substrate. These phenomena, increasing the cell resistance and reducing the transfer rate of charged species, are believed to be the main causes for the poor cycle life of model batteries in high rate discharge tests.

Y.-S. Chen · Y.-Y. Li
Department of Chemical Engineering, National Chung Cheng University, Chia-Yi 621, Taiwan

C.-C. Hu (✉)
Department of Chemical Engineering, National Tsing Hua University, 101, Section 2, Kuang-Fu Road, Hsin-Chu 30013, Taiwan
e-mail: cchu@che.nthu.edu.tw

Keywords Lithium ion battery · Power cell · Cathode · Impedance · Drying temperature

1 Introduction

Because of the higher energy density and other advantages over other batteries, lithium ion batteries (LIBs) are often used as power sources for portable products with extended operating periods, but not as frequently in power-oriented applications. As a result, LIBs were notably absent from power tools and electric vehicles (EVs) in the past, while NiCd and lead-acid batteries occupied almost the entire market. However, due to strict requirements in human health and environment protection, products with toxic or polluting components such as lead and cadmium have been import restricted in several countries. Consequently, most power tool makers have introduced LIBs into their next generation products and the power-type LIBs are also being quickly pushed into the EV/hybrid electric vehicle (HEV) market to replace NiMH batteries or to use directly. Note here that an energy type cell is defined as being used in applications with less than 2 C discharge rates, and a power cell is defined as a battery that can discharge continuously with a current higher than 5 C and pulse discharge higher than 10 C.

Under the above viewpoints, most LIB makers have aggressively developed power cells with a good profit margin, while most LIB studies in the last 20 years have focused on searching for better materials and better compositions to enable a longer cycle life or increase capacity [1–3]. In addition, current leading cell makers only have good experience in producing energy cells. The requirements of power batteries are very different; for example, they must work well at rates higher than 5 C [3–5].

Accordingly, the key factors determining the performance of power cells are certainly different from those for energy cells. Furthermore, their design concept is different from that for energy-type cells, and some new problems not encountered in energy-oriented LIBs must be carefully considered and overcome.

One of the important issues in the performance of power-oriented LIBs is cell impedance and electrode resistance [4, 6, 7]. Note that the commercial LIB power cells presently on the market must cycle well behind 5–10 C and discharge at an extremely high pulse current above 15 C. Based on the above descriptions, cell impedance, which was not well considered in traditional applications under 1 C, has important influences on power cell performance. It is therefore necessary to review (1) the basic concepts of power cell design and (2) quality control even though most parts and materials used in power cells are the same as those used in energy-type cells.

In their efforts to reduce total cell impedance, most LIB makers use thicker substrates, thinner electrodes, highly conductive electrolytes, and a multi-tabs design for power cell design [6]. Since these solutions occupy so much space in the cell, the capacities of commercial power-oriented cells only reach half or 2/3 the capacity of energy-type cells. If a power cell contains a cathode material with a lower specific energy density, such as $LiFePO_4$, then its capacity cannot reach even half that of the present-day energy cells.

This article demonstrates the importance that electrode impedance is a key factor affecting power cell performance. In general, it is possible to copy the geometry of electrode design and electrolyte recipe to make a similar power cell. However, designers usually ignore electrode impedance, which is a significant contributor to the total cell impedance. Although some modeling equations and crucial variables about the impedance of power-oriented LIBs have been discussed and presented in recent articles [7–9], certain issues cannot be suitably expressed in the coin cell scale test. Accordingly, this article investigates the charge–discharge performance of 18650 cylindrical LIB power cells made from cathodes with the same design but produced in different processes.

2 Experimental

This study controls the variable of oven temperature in the drying process for producing electrodes. The cathode recipe is $LiMn_2O_4$/carbon black/PVdF = 96/1.5/2.5 wt%, and the anode recipe is artificial graphite/carbon black/PVdF = 92/1.5/6.5 wt%. The solvent is *N*-methyl-2-pyrrolidone (NMP), and the solid contents for the cathode and anode are 65 and 50%, respectively. The basic electrolyte is a blended solution of PC/EC/DMC = 1/3/6 by weight, 1.2 M $LiPF_6$, and small amounts of additives as SEI formers.

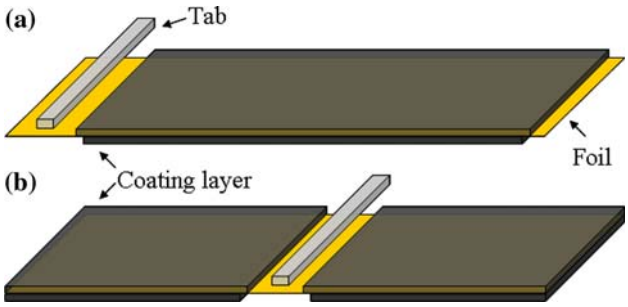

Fig. 1 A scheme for the configuration of **a** conventional and **b** center-tab designs

The battery system in this study is an 18650 (diameter is 18 mm and height is 65 mm) cylindrical cell consisting of a $LiMn_2O_4$ cathode and graphite anode with a 20-μm separator of tri-layer PP/PE/PP (PP: polypropylene, PE: polyethylene). For full cell assembly, a center-tab design that has been used in several commercial cells (see Fig. 1) is applied to lower down the internal resistance, and electrodes with this center-tab design and separators are spirally wound as a cylindrical jellyroll. One difference from an energy-type cell is the positive terminal (header) without a positive thermal coefficient resistor (PTC) inside. Cells were made in a dry room with a controlled dew point lower than −30 °C. The entire procedure for preparing the electrolyte and filling the cells was performed in an Ar-atmosphere glove box with moisture and oxygen contents less than 5 ppm. Cells of the first group consisted of cathodes dried at 115–125 °C (HT-dried cathode), denoted as group A (five cells, A#01–A#05). The second group, with cathodes dried at 100–110 °C (LT-dried cathode), is denoted as group B (five cells, B#01–B#05). The anodes of both group A and group B were produced in the same batch with a LT-drying process. Cells in group C consisted of LT-dried cathodes and HT-dried anodes. Cells from each group were employed in every test, and the data consistency has been well confirmed.

A HP 3478A multimeter was used to measure the dry electrode impedance. An ELCHEMA CM-308 conductance meter was used to obtain the dry electrode conductance. An ADEX AX-1262B Battery mΩ/V m was used to measure the full cell impedance beyond 1 kHz.

3 Results and discussion

The difference in electrode impedance for cathodes made from the same coating slurry but dried at different temperatures is significant (see Table 1). This difference is

Table 1 The impedance and conductance data with the corresponding average cell impedance (ACZ) of dried cathodes prepared in the HT- and LT-drying processes

	HT-drying batch	LT-drying batch
Cathode impedance (Ω)	26.1	13.4
Cathode conductance (S)	0.24	0.42
Full cell ACZ (average by 5) (mΩ)	~15	~13

attributable to the relatively poor dispersion of carbon black in the HT-drying process. Owing to the poor conductivity of $LiMn_2O_4$, the conductance of cathodes must be dominated by the dispersion degree of the conductive diluent which is carbon black here. In this study, the colors of upper layer (face to air) and bottom layer (face to substrate) of cathodes are used to judge the dispersion of carbon black. For the cathode with good dispersion of carbon black, the colors of both upper and bottom layers are very close, which is visible for the LT-dried cathode. For the HT-dried cathode, the the bottom layer is grayish in color, which is close to the color of pure $LiMn_2O_4$, while the color of the upper layer is much darker, indicative of a carbon black-enriched layer. Since the same phenomena were repeatedly found, which cannot be attributed to experimental errors, the lower conductivity of HT-dried cathodes is confirmed to result from the poor dispersion of carbon black. The poor dispersion of carbon black in the HT-dried cathode layer is attributable to a higher evaporation rate of NMP at a higher drying temperature resulting in the floatation of carbon black due to a lower density. The above issue can be improved by increasing the content of carbon black within the active layer if a proper process control is not easy to achieve. However, adding more carbon black in the recipe usually results in more binder because PVdF binder would be occupied by carbon black, which will leave less space for active materials to meet the designed capacity as well as decreasing the safety level.

Table 1 also shows data for the average AC impedance (ACZ) of five full cells consisting of cathodes dried at different temperatures and anodes of the same batch (see cell ACZ). Data in Table 1 reveal that a HT-dried cathode batch exhibits higher impedance than a LT-dried cathode batch, increasing cell impedance. The minor difference in cell impedance (a few mini-ohms) found in Table 1 may not be significant for common energy-type LIBs, but even such a small difference has a huge effect on high power applications (see below).

Figure 2a shows how the small difference in cell impedance in HT-dried and LT-dried cathodes affects the discharge behavior of LIBs. This test analyzes five charge–discharge cycles with a charge rate of 1 C for each cycle. The discharge sequences are 1.5 (1 C), 5, 10, 15 (10 C),

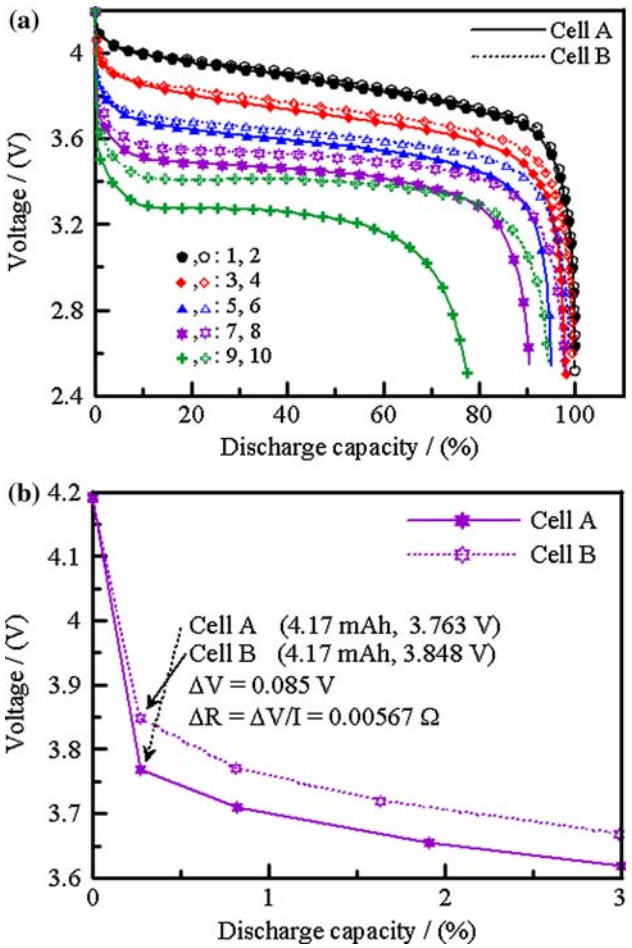

Fig. 2 **a** The discharge curves of (1, 3, 5, 7, 9) cell A#01 and (2, 4, 6, 8, 10) cell B#01 at (1, 2) 1.5; (3, 4) 5; (5, 6) 10; (7, 8) 15; and (9, 10) 20 A. **b** The first-cycle discharging curves of cell A#01 and cell B#01 within the initial 3% discharge capacity under a discharging rate of 15 A

and 20 A. On curves 1 and 2, the cell voltages gradually decrease with the amount of charge delivery, indicating a good intrinsic state of charge for normal Li ion intercalation systems. In addition, the difference between discharge responses for curves 1 and 2 is indistinguishable, revealing that a small difference in cell impedance does not exhibit a significant influence on the performances of LIBs under low discharge rates (i.e., similar to the traditional energy-type case). On the other hand, comparing all the curves in Fig. 2a shows that the differences in discharge capacity and cell voltage become more and more significant as the discharge rate increases. The quasi-linear decay in cell voltage with the charge capacity delivery is also invisible when the discharge rate is equal to or above 10 C (see curves 7–10). Table 2 lists the quantitative rate capacity data for cells A#01 and B#01 deduced from Fig. 2a, where the 1 C discharge capacity in the first cycle is denoted as 100%. The capacities for cell B#01 measured at 15 and 20 A

Table 2 Data of cycled ACZ, DCR_{max}, and discharge capacity for the HT- and LT-drying cathodes ($LiMn_2O_4$) measured at different discharge rates

Cathode	HT-drying (cell A#01)		LT-drying (cell B#01)	
Discharge cycle	Capacity (mAh)	Capacity (%)	Capacity (mAh)	Capacity (%)
C1 (1.5 A)	1,531	100	1,538	100
C2 (5 A)	1,513	98.79	1,531	99.54
C3 (10 A)	1,492	97.43	1,527	99.28
C4 (15 A)	1,450	94.71	1,512	98.31
C5 (20 A)	1,372	89.63	1,488	96.75
Cycled ACZ (mΩ)	28.5		16.0	
DCR_{max} (mΩ)	37.1		29.4	

discharge rates only decrease 30 and 78.6 mAh, respectively. These values are obviously lower than those for cell A#01 (140.4 and 327.9 mAh at 15 and 20 A discharge rates, respectively). The higher capacity loss of group A is due to a higher resistance of the HT-dried cathode. This is confirmed by the larger IR drop of cell A#02 in a continuous 15 A discharging cycling test (see Fig. 2b) since the initial drop in the cell potential is a widely used measure of the ohmic contribution to the cell performance. Figure 2b shows that the initial potential drops of cells A#02 and B#02 on the first-cycle discharge curves are ca. 0.437 and 0.352 V, respectively. Accordingly, the initial resistance difference of cells A#02 and B#02 is ca. 5.67 mΩ, which is close to the difference in the maximum direct-current-resistance (DCR_{max}) values listed in Table 2. All the above results indicate the significant influence of increasing cell impedance using a cathode with a relatively high resistance for power-oriented LIBs.

The difference in the direct-current-resistance (DCR) of cells A#01 and B#01 (e.g., see the DCR_{max} values listed in Table 2) is consistent with the evidence of AC-impedance. This study estimates the DCR on the basis of Ohm's Law (see Eq. 1):

$$R = |\Delta V/\Delta i| \quad (1)$$

According to Ohm's Law, the DCR can be obtained at each discharge capacity from the 1.5–20 A discharge data. Note that the DCR_{max} of cells A and B occurs at approximately 10–12% delivery of cell capacity, at 150–180 mAh. In addition, the DCR difference between cells A#01 and B#01 gradually increases from ca. 7.0 to 7.7 mΩ with the delivery of cell capacity. Also note the higher resistance of group A, which indicates lower power production at the same current. This loss of power due to higher cell impedance is transformed into heat that causes a rapid rise in cell temperature during the extremely high rate discharge process, which is one of the main reasons responsible for its poor cycle life (see below).

Another significant difference in Table 2 is the cell AC-impedance after the five-cycle charge–discharge test, which is denoted as cycled ACZ. In general, cell ACZ should increase smoothly and slowly under the normal charge–discharge cycling. It is therefore not reasonable to expect such a high raise in cell ACZ of cell A#01 after only a few charge and discharge cycles. This unusual behavior is attributable to (1) the cell heating during the extremely high rate discharging process and (2) poor cathode conductivity.

The relatively poor conductivity of HT-dried cathodes may arise from inadequate contact of the active material particles. This in turn is caused by poor adhesion of the binder at higher temperatures, especially when using a larger weight percentage of binder. In fact, the adhesion of cathodes and anodes had been confirmed to meet the adhesion requirements of commercial LIBs. The binder content of all cathodes in this study is based on the design of commercial products, which is quite low compared with laboratory compositions. Therefore, the temperature range of HT-drying, 115–125 °C, should be not high enough to cause poor adhesion or other negative effects on the cathodes. This idea is supported by the fact that there is no adhesion issue in the HT-dried anodes (see below) because anodes have higher binder content. Accordingly, the relatively poor conductivity of the HT-dried cathodes is more likely attributable to the poor dispersion of carbon black. The dispersion of carbon black may be improved by increasing the carbon black content within the active layer if the HT-drying process is used to manufacture cathodes for power-oriented LIBs. However, a cathode recipe of high carbon black content usually requires more PVdF binder. This increase in both carbon black and PVdF contents leaves less space for $LiMn_2O_4$, which fails to meet the designed capacity and reduces the safety level of LIBs.

Cell heating during the extremely high rate discharging process may melt down the porous, meltable separator widely used in current LIBs and interrupt the transport of charged species. When pores gradually close during the discharging process, the cell impedance corresponding to the movement of ions within the separator becomes higher and higher. As a result, cell ACZ also increases gradually.

Cell heating also causes the cathode to peel from the aluminum substrate under high temperature environments. Observations of the disassembled cells A#01 and B#01 after the five-cycle test reveal that more area of the coated cathode in cell A#01 detached from the substrate (attached to the separator) compared to cell B#01. This peeling phenomenon also makes the charge transfer more difficult and creates higher impedance. The poor conductivity of the cathodes is due to poor electronic conductivity of $LiMn_2O_4$. Since all electrochemical tests show that the electrode conductivity easily interferes with the discharge performances, this effect is more significant for LIBs in the high power applications. The factors mentioned above are responsible for the rapid rise in ACZ within only five charge and discharge cycles. The heating effect on the separator ionic conductivity and cathode peeling from the substrate is predominant in this study because the cell skin temperature exceeded 80 °C during the 20 A discharging process. The real temperature near the cathode tab inside the cell should be much higher (even higher than 100 °C). Hence, the lower porosity of a used separator and the increased cathode peeling area due to cell heating give the best explanations for the rapid increase in cycled ACZ. On the other hand, the rate of Mn dissolution will be enhanced under a high temperature environment, which may be plated on the anode to increase cell impedance [10]. However, this effect is not considered as the main reason responsible for the rapid increase of the ACZ impedance because the test employed here comprises only five cycles.

Figure 3 shows the continuous 15 A discharge-cycling characteristics of cells A#02 and B#02 between 4.2 and 2.5 V with a 1.5 A charging rate. The cycle life of cell A#02 is quite poor under this test, while the cycle life of cell B#02 with low impedance is comparatively much better. Cell A#02 failed at the 25th cycle and cell B#02 worked over 120 cycles, revealing a huge gap in cycle life between the two models. This phenomenon is reasonably attributable to extra heat generated by the power loss created by higher impedance in the extremely high rate discharge process. This heat generation causes a rapid rise in cell temperature and closes pores in the meltable separator (see below), and even accelerates the degradation of $LiMn_2O_4$ [11, 12]. The influence of Mn dissolution resulting in the Mn deposition onto anodes should be more significant in this longer cycling test.

The statement above is supported by the significant difference in cell temperatures during the charge–discharge cycling test in Fig. 4. Figure 4 shows the maximum skin temperature (T_{max}) at each cycle of both cells. The power dissipation at a constant discharge current (15 A here) can be calculated according to the equation of modified power consumption expressed below:

$$\Delta P = I^2 \times \Delta R \quad (2)$$

The DCR profiles of groups A and B (not shown here) show that the waste power coming from the difference in cell impedance can be calculated; about 27% extra power appears in heat form in group A. This heat generation rate is high enough to cause the different T_{max} in each cycle between cells A#02 and B#02 under the 10 C discharge rate (see Fig. 4).

Cell A#02 failed at the 25th cycle under a 15 A discharge cycling test, which is attributable to power dissipation causing a rapid rise in cell temperature. This rapid rise in cell temperature due to power dissipation exhibits an additional effect: pore closure in the meltable separator. A comparison of the separators disassembled from cell A#02 after the 25-cycle, 15 A-discharge test (Fig. 5a) with a fresh one (A#04, Fig. 5b) confirms that this effect causes pore closure in the meltable porous tri-layer PP/PE/PP

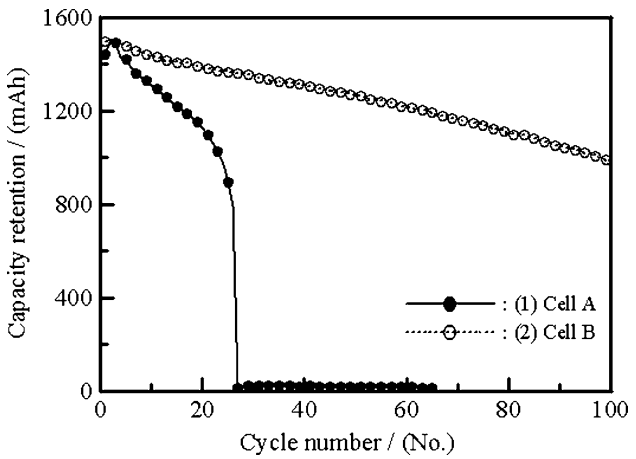

Fig. 3 Capacity loss against cycle number in a 1.5 A charge–15 A discharge test for (*1*) cell A#02 and (*2*) cell B#02

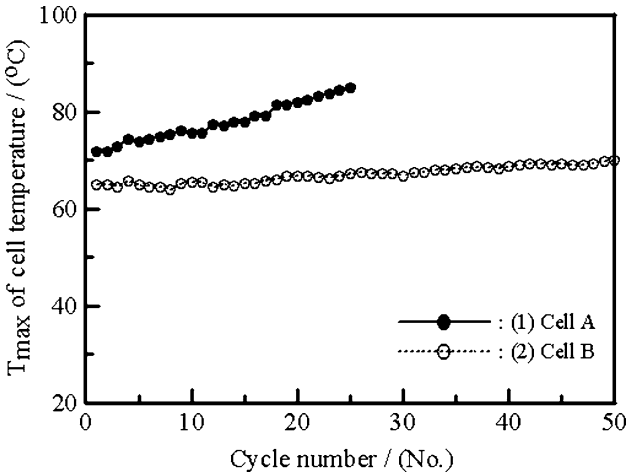

Fig. 4 The maximum skin temperature against cycle number in a 1.5 A charge–15 A discharge test for (*1*) cell A#02 and (*2*) cell B#02

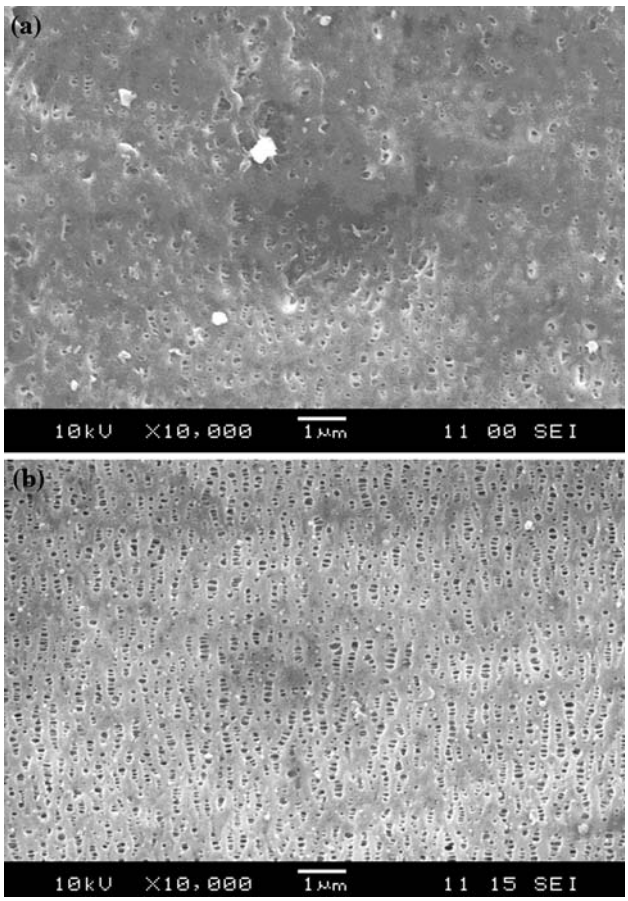

Fig. 5 SEM images of a tri-layer PP/PE/PP separator from **a** cell A#02 after and **b** A#04 before the 1.5 A charge–15 A discharge cycling test employed in Fig. 3

separator. It is very clear that the extra heat generation from power dissipation in cell A#02 during the 25-cycle, 15 A-discharge test closed most pores within the polymer separator by melting. This phenomenon interrupts the transport of charged species and strongly supports the impact of cell heating on the rapid increase in cycled ACZ discussed previously. Note that this quick increase of cell ACZ still stays within the normal range of energy-oriented cells. This is because the pores in the separator were not totally closed. This phenomenon created many channels inside the separator, producing a lower ACZ than that of a cell with a total pore-closing separator. However, this increase in ACZ has a significant impact on the high rate discharge, the most important function of a power cell. Accordingly, the cell heating resulting from the loss of power due to higher cell impedance in the extremely high rate discharge process is concluded to be, at least, one of the main reasons responsible for the poor cycle life of cell A#02.

The above results and discussion show that while the influence of electrode resistance on LIB performance in high rate discharge applications is significant, this effect is not obvious for low rate discharge applications. Figure 6 compares continuous 1.5 A (1 C) charging–discharging results between 4.2 and 2.5 V for cells A#03 and B#03. The profiles of both cells are very similar, indicating an insignificant influence of electrode impedance under such a relatively low rate. There is almost no difference in skin temperature between cells A#03 and B#03, and the rate of increase in skin temperature is very slow. At the end of 1 C discharge (about 1 h), the cell skin temperature increased less than 4 °C for each cell. This minor increase in cell temperature does not cause a serious fade in performance. This result suggests that the low heat generation rate is close to the heat flux (conduction and convection) in the atmosphere, causing only a small difference in skin temperature. Unfortunately, a 1.5 A discharging rate is not typical for power-oriented LIBs, and a 10–15 A cycling ability is a more common judgment criterion.

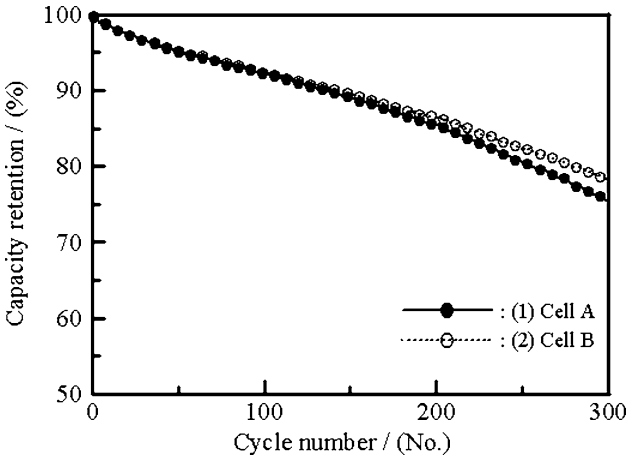

Fig. 6 Capacity loss against cycle number in a 1.5 A charge–discharge test for (*1*) cell A#03 and (*2*) cell B#03

This article also studies the effects of anodes produced in the HT- and LT-drying processes since the drying temperature of cathodes has been demonstrated to cause a huge impact on high power performance. The dry electrode impedances of HT- and LT-dried anodes are 0.16 and 0.15 Ω, respectively, which are almost the same and very close to the sensitivity limit of the measuring instrument. Table 3 shows that the electric properties of cell C#01 consist of a HT-dried anode and a LT-dried cathode, as a reference to cell B#01 in Table 2. According to this table, the DCR profiles (not shown here), and the discharge curves (not shown here), the HT-dried anode also causes higher cell impedance and cycled ACZ (similar to the case of a HT-dried cathode). However, its impact is much lower than that of a HT-dried cathode. The reason for this minor impact is reasonably due to the good electrode conductance of graphite anodes used in both cells. Graphite conductance is far superior to that of metal oxides (specifically, spinel

Table 3 Data of cycled ACZ, DCR_{max}, and discharge capacity for cell C#01 measured at different discharge rates

Anode	HT-drying (cell C#01)		LT-drying (cell B#01)	
Discharge cycle	Capacity (mAh)	Capacity (%)	Capacity (mAh)	Capacity (%)
C1 (1.5 A)	1,540	100	1,538	100
C2 (5 A)	1,531	99.42	1,531	99.54
C3 (10 A)	1,525	99.03	1,527	99.28
C4 (15 A)	1,508	97.92	1,512	98.31
C5 (20 A)	1,483	96.30	1,488	96.75
Cycled ACZ (mΩ)	17.6		16.0	
DCR_{max} (mΩ)	30.1		29.4	

$LiMn_2O_4$ in this study). Contrary to graphite with good conductivity, the cathode conductance is very poor if no conductive carbon black particulates are mixed with these metal oxide powders. Accordingly, the graphite anode still shows good conductance and creates less of an impact on cell performance even though the carbon black is not well dispersed in the HT-drying process. Based on the above data and discussion, the high rate cycle life of a power cell with a HT-dried anode should be close to that of the cell with a LT-dried anode.

After demonstrating the importance of cathode impedance in the high power applications, this article finally investigates the charge–discharge-cycling behavior of energy-type LIBs with cathodes produced in both HT- and LT-drying processes (denoted as groups D and E, respectively). The energy-type LIBs employed here are $LiCoO_2$-graphite 2.2 Ah 18650 cells. Owing to the different considerations for power- and energy-oriented cells, the electrode formulation, cell design, and electrolytes of these energy-type LIBs are different from those of the power-type cells. However, all the materials and parts were kept the same for both energy-type cells with the exception of cathodes which were prepared in different drying processes. Since energy cells used in most laptops are required to work for at least 2 h, a 0.5-C cycle life was employed as an index for judging cell performance. Figure 7 shows the typical continuous 0.5 C (1.1 A) discharge-cycling characteristics of cells D#01 and E#01 (at 1.54 A charging rate) between 4.2 and 2.5 V. Comparison of curves 1 and 2 in Fig. 7 shows that the difference in discharge capacity caused by different cathode impedance for each discharge test is not significant during the first hundred cycles. In addition, only about a 2% difference in capacity loss between cells D#01 and E#01 appears after the 200-cycle charge–discharge test (i.e., the discharge time difference is only 2–3 min in the 0.5 C discharge test). Unlike the huge impact on the high rate capabilities of LIB power cells, the impact of cathode impedance on the low rate discharge capability of energy-type cells is minor and negligible. Accordingly, the HT-drying process can be used to manufacture cathodes for energy-type cells to shorten the processing period and to promote throughput, since the performance of group D is still much better than user requirements.

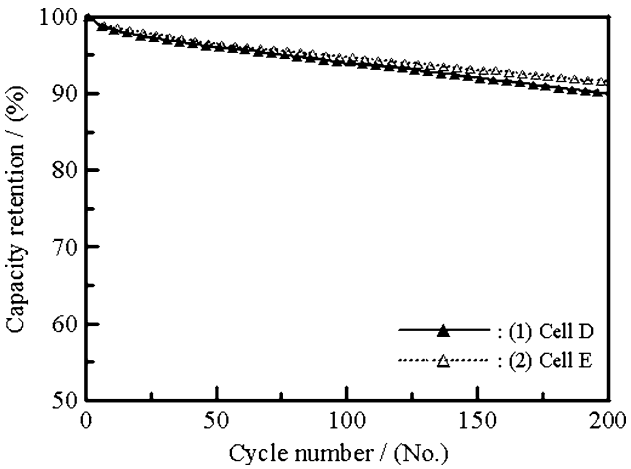

Fig. 7 Capacity loss (in percentage) against cycle number in a 0.5 C discharge rate test for (*1*) cell D#01 and (*2*) cell E#01 (the energy-type $LiCoO_2$-graphite 2.2 Ah 18650 cells)

4 Conclusions

This study successfully demonstrates how a small change in cathode preparation affects the high-rate discharging characteristics of LIB power cells due to a small variation in the cathode impedance. A cathode dried at the wrong temperature exhibits relatively high impedance, resulting from poor distribution of carbon black particulates over the oxide powders. This relatively high impedance not only reduces its high-rate discharging performance but also generates extra heat by power dissipation, which leads to a poor high rate cycle life. Cell heating during an extremely high rate discharging process causes pore closure of the porous separator and cathode peeling from the substrate, further increasing the cell resistance. Hence, the cycle life

of a power-oriented battery pack comprising cells with relatively high impedance cathodes will be much shorter because power dissipation generates more heat in the charging–discharging cycles, activating the temperature protection circuit earlier.

Acknowledgment The financial support of this study, by the National Science Council of ROC under contract no. NSC 97-2221-E-007-078 and the NTHU boost program, is gratefully acknowledged. The support of cell manufacturing by E-one Moli Energy Corp. is highly appreciated.

References

1. Zhong Q, Bonakdarpour A, Zhang M, Gao Y, Dahn JR (1997) J Electrochem Soc 144:205
2. Saitoh M, Sano M, Fujita M, Sakata M, Takata M, Nishibori E (2004) J Electrochem Soc 151:A17
3. Bloom I, Jones SA, Battaglia VS, Henriksen GL, Christophersen JP, Wright RB, Ho CD, Belt JR, Motloch CG (2003) J Power Sources 124:538
4. Abraham DP, Reynolds EM, Schults PL, Jansen AN, Dees DW (2006) J Electrochem Soc 153:A1610
5. Horiba T, Maeshima T, Matsumura T, Koseki M, Arai J, Muranaka Y (2005) J Power Sources 146:107
6. Rimers JN (2006) J Power Sources 158:663
7. Dees D, Gunen E, Abraham D, Jensen A, Prakash J (2005) J Electrochem Soc 152:A1409
8. Dokko K, Mohamedi M, Umeda M, Uchida I (2003) J Electrochem Soc 150:A425
9. Abraham DP, Poppen SD, Jensen AN, Lin J, Dees DW (2004) Electrochim Acta 49:4763
10. Amine K, Liu J, Belharouak I, Kang S-H, Bloom I, Vissers D, Henriksen G (2005) J Power Sources 146:111
11. Gao Y, Dahn J (1996) J Electrochem Soc 143:1783
12. Yamane H, Inoue T, Fujita M, Sano M (2001) J Power Sources 99:60